# Impact of using selective collector bar rodding on the MHD stability of a 500 kA aluminium electrolysis cell

M. Dupuis
*GéniSim Inc.*
*3111 Alger St.*
*Jonquière, Québec, Canada G7S 2M9*
*marc.dupuis@genisim.com*

V. Bojarevics
*University of Greenwich, School of Computing and Mathematics*
*Park Row*
*London, SE10 9LS, UK*
*V.Bojarevics@gre.ac.uk*

## ABSTRACT

It has been previously demonstrated [1,2] that using selective collector bar rodding has a big impact on the uniformity of the current density at the top surface of the cathode block and hence on the intensity of the horizontal current in the metal pad.

The present study investigates the impact of using selective collector bar rodding on the MHD stability of a 500 kA aluminium electrolysis cell. For this purpose the recently developed MHD package for the aluminium reduction cell time dependent behavior is used.

## INTRODUCTION

Since the introduction of 100% graphitic cathode block in the high amperage cell, their fast erosion rates have lead to a significant reduction of the average cell life. Furthermore, the observed "W" shape erosion pattern [3] implies that that erosion rate is proportional to the current density at the metal/cathode block interface.

Considering those facts, it has been proposed in [1] to use selective collector bar rodding in order to get a more uniform current density at that interface. This was successfully achieved without significantly increasing the cathode voltage drop by using bigger collector bars.

Of course, as demonstrated in [2], having a uniform current density at the metal/cathode block interface also almost completely eliminates the horizontal currents in the metal pad. This in turn should have a significant impact on the MHD cell stability. In order to be able to analyze that impact, the MHD model must be able to represent the selective cast iron rodding pattern around each collector bar.

## SELECTIVE RODDING PATTERN

The selective rodding pattern used in the present study is similar to the one presented in reference (1) (see Figure 1). The rodding of each collector bar is split in three sections of decreasing size while going from the center of the cell side wall. The length of the middle section is half of the section close to the cell center while the section close to the cell wall is about one third of the middle section. The resulting current density in the metal pad obtained using the ANSYS® based thermo-electric model is presented in Figures 2.

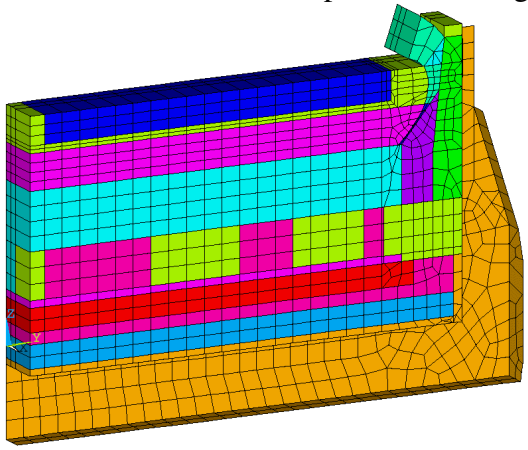

Figure 1: Selective rodding pattern

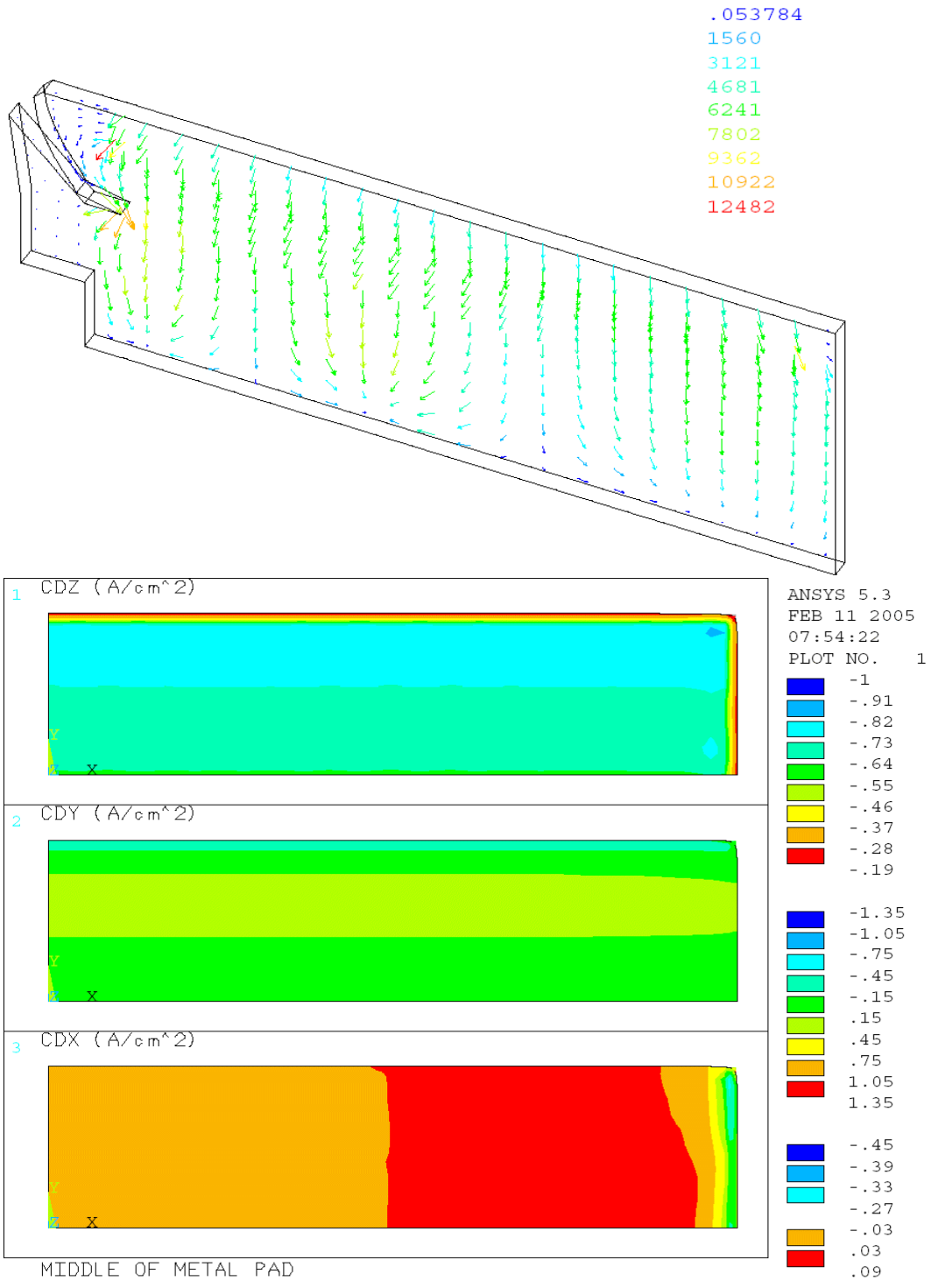


Figure 2 - Resulting current density in the metal pad obtained using the ANSYS®

## MHD COMPUTATIONAL MODEL

The design of bus network for high amperage reduction cells has a double fold task: to optimize the magnetic field within the cell and the electric current distribution both within the cell and the bus bars itself. The magnetic field should be reduced and optimized for a stable melt interface and to avoid vigorous velocities within the liquid melt. Since the magnetohydrodynamic driving force is **j**x**B**, the electric current distribution, particularly the horizontal components, are equally important to the magnetic field optimization.

Historically two different modelling approaches have been used: one for the electric current distribution for the bus bar network and, often quite different, other mathematical model for the MHD phenomena within the cell. Very similar data inputs both for the magnetohydrodynamic simulations and for the electric current modeling in the bus network are in fact used. Physical and engineering considerations suggest that both problems are mutually interconnected and should be solved interactively. It means that the computer program should use the same data input to compute the electric current, voltages, temperatures in the bus network, and the magnetic field, the current distribution within the cell with waving metal interface, then finally iterate back to account for the spatially and temporally variable cell interpolar distance for the current distribution in the supplying bus network. This affects also the magnetic field, the metal pad waves, velocities, and the neighbor cells which are interconnected to the particular test cell (4-6).

### Electric Current Distribution

The first calculation step needed for an MHD model is the electric current distribution. This is calculated by coupling the electric current in the fluid zone to the resistance network representing the elements of individual anodes and cathode collector bars as well as the whole bus-bar circuit between two adjacent cells. The electric current in the fluid zones must be computed from the continuous media equations governing the DC current (which can change in time with the waves and anode burnout process):

$$\mathbf{j} = -\sigma\nabla\varphi + \sigma\mathbf{v}\times\mathbf{B}, \tag{1}$$

where the fluid flow induced currents in the highly conducting liquid metal are accounted for. The electric potential in the fluid is governed by the equation:

$$\nabla^2\varphi = \nabla\cdot(\mathbf{v}\times\mathbf{B}), \tag{2}$$

and the boundary conditions of zero current at the insulating walls, given current distribution $\mathbf{j_a}$ at anodes, $\mathbf{j_c}$ at cathode carbon (both supplied from the finite element resistivity network

solution, which in turn is coupled to the computed potential distribution from the equation (2) ). At the interface between the liquid metal and the electrolyte the continuity of the potential and the electric current normal component must be satisfied. Since the depths of the liquid layers are extremely small if compared to their horizontal extension, the shallow layer approximation is very efficient to solve this 3-dimensional problem. It can be shown (7) that the solution, for instance in the aluminium layer, can be obtained from the following equation:

$$j_{za}(x, y, t) - j_{zc}(x, y, t) = \sigma_{Al}\partial_k((H_{Al}(x, y, t) - H_c)\partial_k\varphi), \qquad (3)$$

Where the aluminium pad interface $H_{Al}$ is variable in time and horizontal coordinates, and the current distribution at the top and the bottom depend on the iterative solution from the finite element network of the bus bars, anodes, pins, collector bars and the collector bar rodding procedure (see e.g. Figure 1).

As the beginning of the computer simulation the MHD package generates automatically a very large set of Kirchhoff equations from the relatively simple unified data input. The current distribution in the bus bar network can be described to reasonable approximation accuracy suitable for engineering purposes by linear resistance elements. The electric currents and voltages in such a complex, multiply connected circuit are governed by the Kirchhoff laws. The two Kirchhoff laws are:

1) the **voltage law**: The algebraic sum of the potential differences taken around a loop (or 'mesh') of a circuit is zero;

2) the **current law**: The algebraic sum of the currents into a node of a circuit is zero.

If directly applied, these laws contain unknown potential differences for each resistance and unknown currents for each mesh of a given circuit. There are two methods to reduce the number of independent unknowns and the equations respectively. These are based on combining the two laws and are referred to as either mesh analysis or nodal analysis.

The mesh analysis is based on currents as unknowns. A set of mesh currents $I_n$ are chosen to traverse all complete loops of the circuit. Since each mesh current flows right through any junction (node) in its path, the current law is automatically satisfied. Then it is left to apply the voltage law for each of the meshes by replacing the potential differences with the algebraic sums of currents through the particular resistance multiplied by this resistance (Ohms law). For the reduction cell situation this procedure was used in the past and involves a tedious job of locating all possible meshes of the circuit, what is rather hard to automate in a computer program. Therefore this approach involves an intelligent input from the program user and results in long labor days with a possibility of potential errors. Principal changes in the circuit, such as anode or cathode element disconnection or new branching, require significant reconsideration of the equation set.

For the automatic circuit analysis purpose the nodal analysis is more convenient. According to this method the potentials at the nodes are the independent unknowns. The use of node potentials, rather than mesh currents, makes for greater efficiency in the analysis of circuits that are predominantly running in parallel to other branches, since the number of simultaneous equations that have to be solved is significantly smaller. The general procedure to obtain the equation set for a complex circuit is the following:

1) choose a convenient reference (given potential for a set of nodes - in our case the liquid metal of the previous cell where the internal electric current distribution is computed in the liquid layers) and assume a potential (unknown before the solution) for all remaining nodes;

2) in the equation for a particular node, the known coefficient at the potential of that node is the sum of the conductances (inverse to resistances) connected to it; the coefficients of the other potentials are the conductances joining their respective nodes to the node in question;

3) this algebraic sum of potentials multiplied by conductances is equal to an external current entering this node.

The following equation set arises for the total number of *M* nodes each of which has *N* directly connected neighbor resistances:

$$U_m \sum_{n=1}^{N} \frac{1}{R_n} - \sum_{n=1}^{N} \frac{U_n}{R_n} = I_m \quad , \tag{4}$$

where $U_m$ is the potential at a node, $U_n$ - for nodes at other ends of neighbor bars, $R_n$ - resistances of neighbor bars, $I_m$ - external current entering the node. In our case total current 'I' enters the reference nodes in the liquid metal of previous cell and '-I' current leaves the nodes at the liquid metal of the downstream cell. For all other nodes the external current - right side of the equation - is zero.

This is just another statement of the current law, and the voltage law is satisfied because the sum of the potential differences, with $U_m$ expressed from the equation (4), over the closed mesh is identically zero. Formally this law can be applied even for two resistance elements connected in series, and this property is essential in order to generate automatically the set of equations to solve.

After finding the potentials at the nodes, the potential difference between two neighbor nodes multiplied by the connecting resistance gives the current in each resistance. The main task of the present program is to find the current distribution in the bar network, yet a further improvement in accuracy can be achieved if computing Joule heating: $R_m \ I_m^2$ for each of the resistance elements.

Knowing the Joule heating, losses to the ambient air and the connectivity of the bars, it is possible to estimate the temperature of a bar. When the temperatures are calculated, the resistivities $\rho_T$ can be updated taking into account the linear temperature coefficient $\alpha$ :

$$\rho_T = \rho_{20} \cdot (1+\alpha T). \tag{5}$$

After the new resistances are calculated, the electric circuit equation set is solved again to iterate the whole procedure while the convergence is achieved. The convergence is easily established for bars with physically reasonable cross sections and sufficiently effective heat transfer to the ambient air and to the neighbor bars. We incorporate in the program also the heating at the ends of first and last bars connected to the anodes and the cathode carbon by assigning the temperatures at these ends. The computed temperatures of the electrically heated bars permit to accommodate to the resistivity changes. The described procedure is sufficiently flexible to permit simulation of anode changes, disconnected cathode bars, various branching of the current path between the cells, etc. The procedure is also well suited to model the selective rodding of the collector bars as shown in Figure 1.

## MHD MODELLING RESULTS

The MHD simulation package provides time dependent results for a specified bus bar network shown in Figure 3 for an experimental new design 500 kA cell (4-6). The bus bar design achieves a high level of MHD stability for the 500 kA cell, but certain problems are encountered, as it is often the case, for the cells close to the line beginning and end. Small amplitude oscillations persist for these cells. Therefore we attempted to analyze the MHD stability for the cells close to the line end as shown in Figure 3.

First, we consider the cell behavior without the selective rodding and with the simple case of uniform 20 cm ledge covering the cathode carbon along the cell bottom perimeter. (More realistic case with the ledge obtained from the thermoelectric modelling is considered in (6).) The electric current distribution, computed according to the coupled model given by the equations (1)-(5), is shown in Fig. 4, where the arrows indicate the horizontal depth average current in metal and the contour levels – $J_z$ current at the bottom.

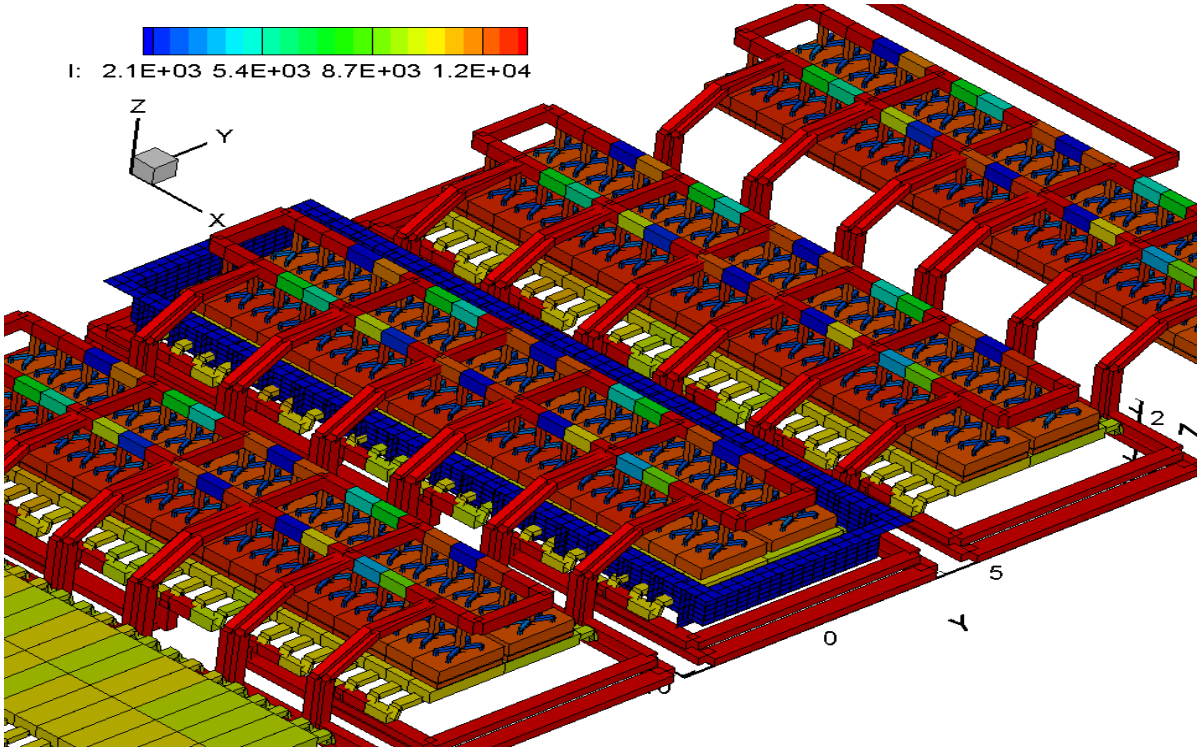


Figure 3 – The bus bar network and the electric current distribution for the 500 kA cell positioned close to the line end. The test cell contains also the ferromagnetic parts for the magnetic field prediction

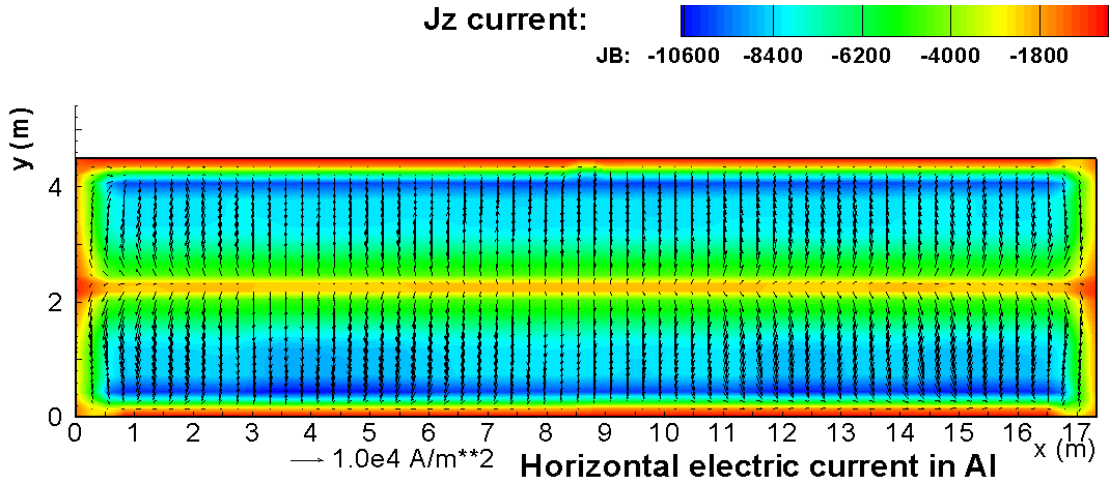


Figure 4 – Electric current distribution in the aluminium layer for the standard case without selective collector rodding

For the end cells the metal pad develops low amplitude self-sustained, non-growing oscillation, which is visually hardly noticeable (compare Figures 5 and 6, showing the pad surface at time moments separated by a half-period of the oscillation: max and min height for a particular location). Notice, that the maximum amplitude is just a few millimeters, and that relatively intense horizontal circulation velocities are mainly responsible for the interface deformation in this case. Figures 7 and 8 show the depth-average velocity distribution in both liquid layers. The 'dips' in the interface are created by the more intense bottom layer vortex velocities (the right and middle parts), and the 'crest' of the surface is largely supported by the pressure reduction owing to the more intense electrolyte vortex on the left part.

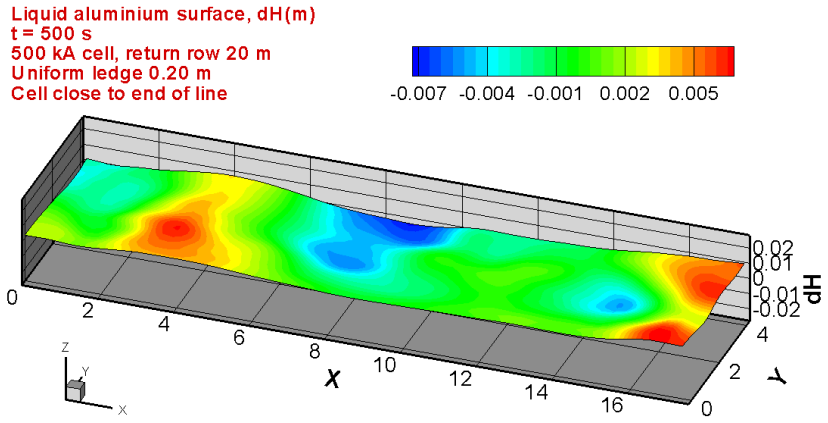


Figure 5 – Liquid metal pad instantaneous surface at 500 s for the standard case without selective collector rodding

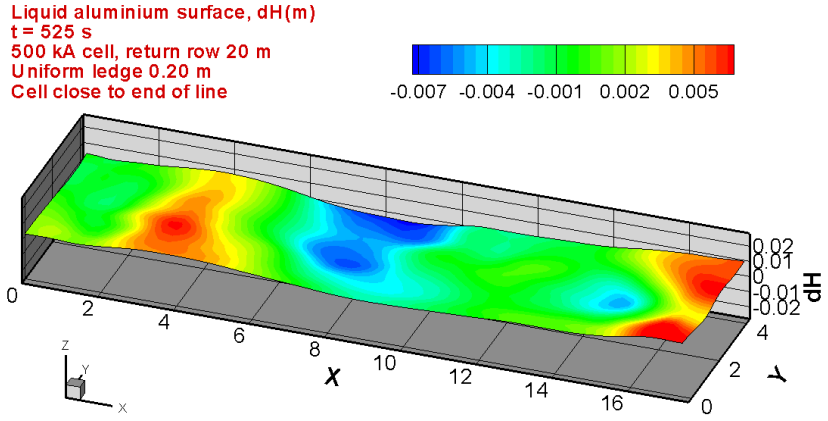


Figure 6 – Liquid metal pad instantaneous surface at 525 s for the standard case without selective collector rodding

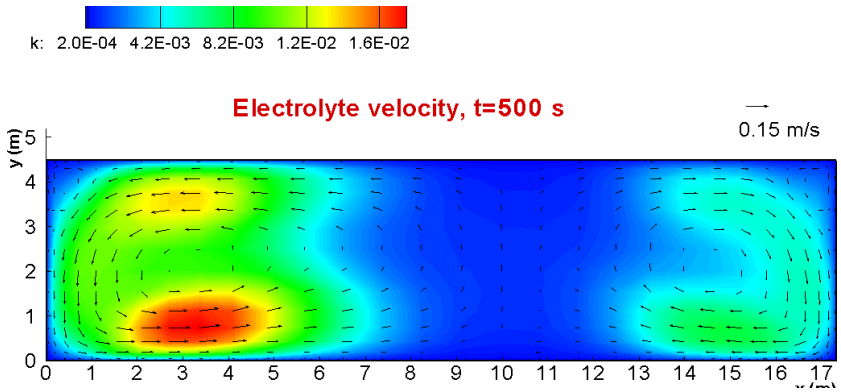


Figure 7 - Velocity pattern and turbulent kinetic energy k distribution in the electrolyte layer for the standard case without selective collector rodding

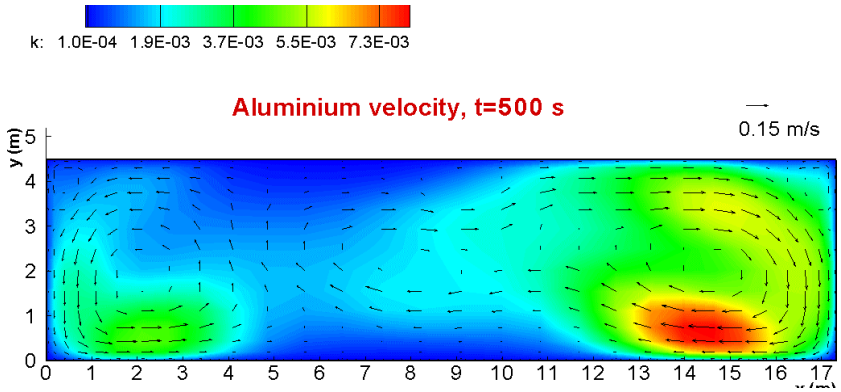


Figure 8 - Velocity pattern and turbulent kinetic energy k distribution in the aluminium layer for the standard case without selective collector rodding

The metal pad surface oscillation indicates (see Figure 9) a mild instability developing over a very long time period for the case of the end cells. The middle of the line cells are very stable even without any additional stabilizing measures. For the end cells we attempt to introduce the selective collector bar rodding (shown in Figure 1) in order to reduce the horizontal currents in the metal pad. The MHD model is more sensitive to the 3-dimensional nature of the external bar connection, which leads to clearly visible bottom current increase at the metal bottom where the rodding is applied. The resulting horizontal currents in the metal are indeed considerably reduced (Figure 10). The horizontal velocity patterns are changed, also, and made almost similar in both liquid layers (Figures 11 and 12). The metal pad surface is more flat (Figures 13 and 14) than without the selective collector

bar rodding (compare to Figures 5, 6). The small 'dips' seen in the Figures 13, 14 are created because the aluminium vortices are slightly more intense than in the electrolyte for this case.

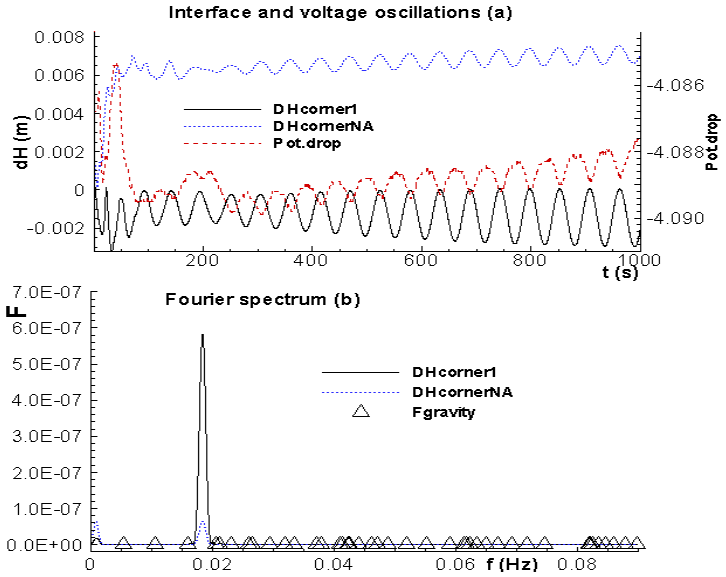


Figure 9 – (a) Liquid metal pad and cell voltage oscillations for the standard case without selective collector rodding; (b) Fourier power spectra for the pad oscillations.

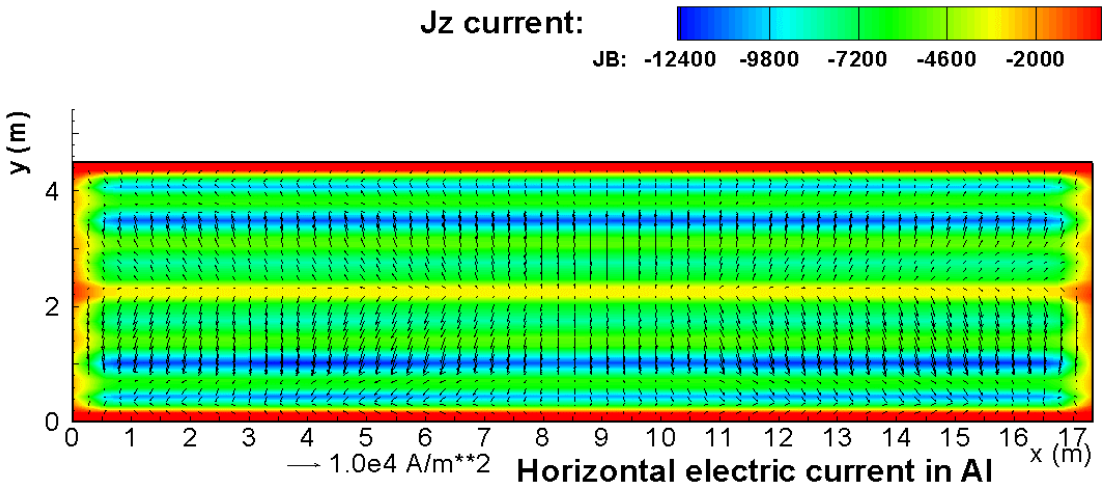


Figure 10 – Electric current distribution in the aluminium layer with selective collector rodding

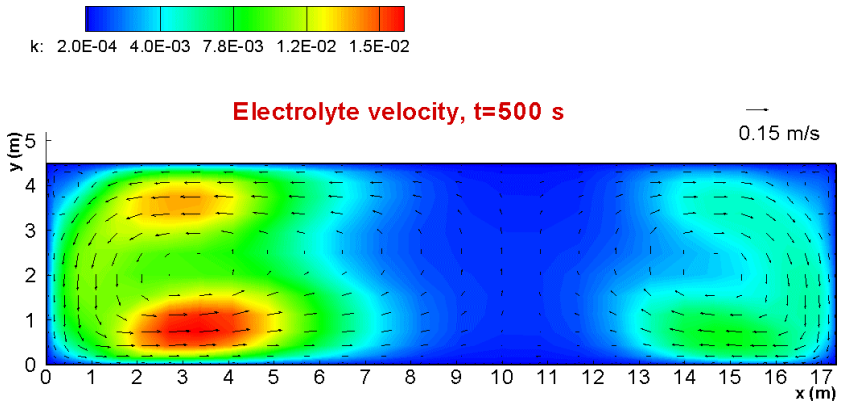


Figure 11 - Velocity pattern and turbulent kinetic energy k distribution in the electrolyte layer for the case with selective collector rodding

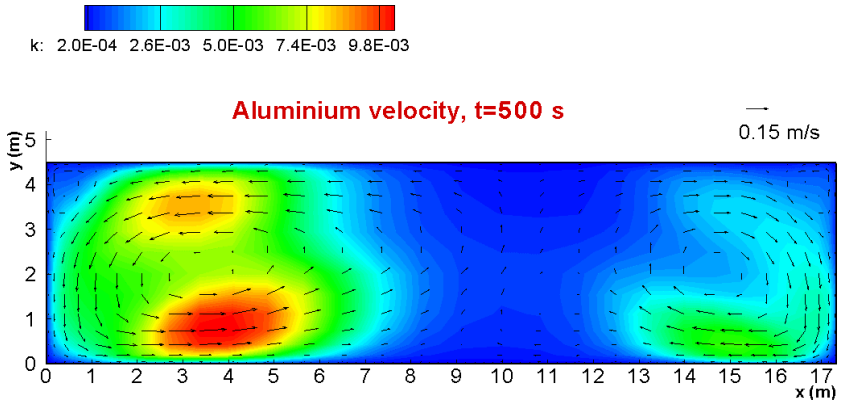


Figure 12 - Velocity pattern and turbulent kinetic energy k distribution in the aluminium layer for the case with selective collector rodding

The metal pad surface oscillation still exists, however not growing after a rather long time period simulated (Figure 15) , because the magnetic field $B_z$ component for the end cells is about 14 Gs on average if compared to 8 Gs for the cells in mid-line where a high level of MHD stability is achieved (see Figure 16). The cell voltage oscillations shown additionally in Figures 9 and 15 indicate similar oscillations, which can be easily detectable from the overall cell voltage measurements. The average voltage is decreasing in magnitude by 1-2 mV during the course of the simulation in both cases because of the gradual anode burnout process incorporated in the model which makes the average ACD more uniform, reduces the overall cell resistivity and stabilizes the cell noise produced by the MHD waves.

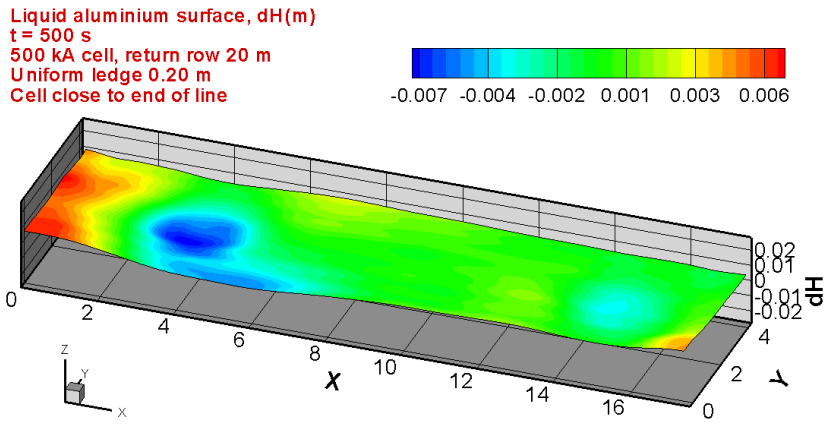


Figure 13 – Liquid metal pad instantaneous surface at 500 s with selective collector rodding

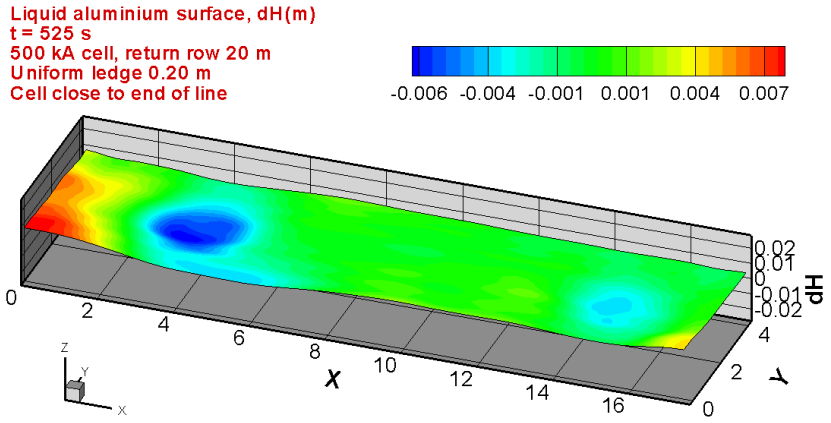


Figure 14 – Liquid metal pad instantaneous surface at 525 s with selective collector rodding

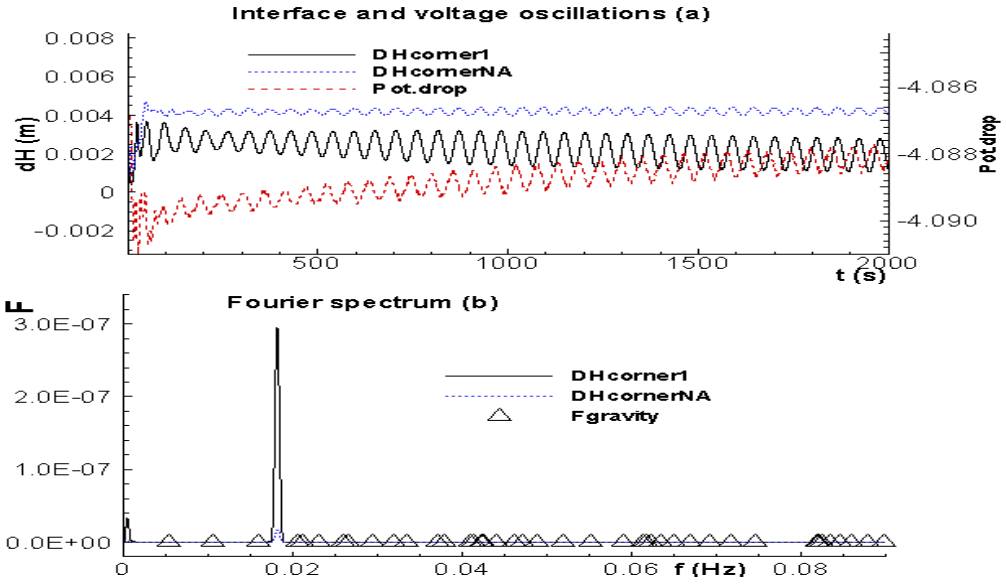


Figure 15 – (a) Liquid metal pad and cell voltage oscillations for the case with selective collector rodding; (b) Fourier power spectra for the pad oscillations

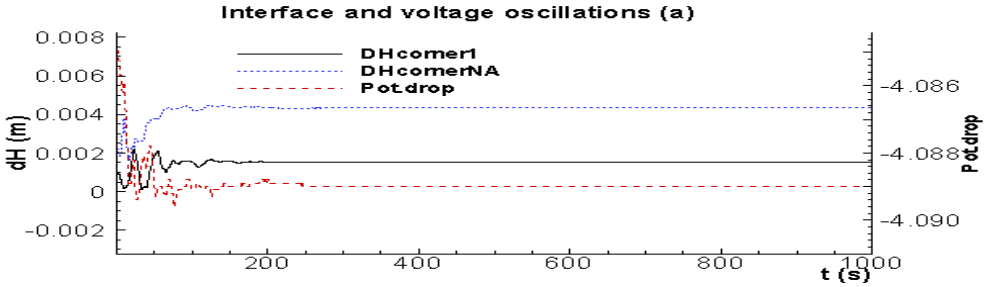


Figure 16 – Liquid metal pad and cell voltage oscillations for the case with selective collector rodding when the cell is located in the middle of the line

## CONCLUSIONS

The MHD stability modelling for the experimental high amperage 500 kA cells indicates that the selective collector bar rodding can be useful for reducing the cell noise and increasing the stability. The effect may be particularly useful for the end of line cells where the stability is often compromised.

## REFERENCES


1. Dupuis, M., Development of a 3D transient thermo-electric cathode panel erosion model of an aluminum reduction cell, CIM Light Metals, 2000, 169-178.

2. Dupuis, M., Computation of accurate horizontal current density in metal pad using a full quarter cell thermo-electric model, CIM Light Metals, 2001, 3-11.

3. Reny, P. and Wilkening, S., Graphite Cathode Wear Study at Alouette, Light Metals, TMS, 2000, 399-404.

4. M. Dupuis, V. Bojarevics and J. Freibergs, Demonstration Thermo-Electric and MHD Mathematical Models of a 500 kA Al Electrolysis cell, Proceedings of the 42nd Conference on Light Metals, CIM, 2003, 3-20.

5. M. Dupuis, V. Bojarevics and J. Freibergs, Demonstration Thermo-Electric and MHD Mathematical Models of a 500 kA Al Electrolysis cell, Part 2, Light Metals 2004, Ed. Alton T. Tabereaux,TMS, 2004, 453-459.

6. M. Dupuis and V. Bojarevics, Weakly coupled thermo-electric and MHD mathematical models of an aluminium electrolysis cell, Light Metals 2005, Ed. Halvor Kvande, TMS, 2005, 449-454.

7. V.Bojarevics, Interfacial MHD waves and associated heat distribution due to the dynamic electric current interaction in an aluminium electrolysis cell. Recent Advances in Heat Transfer, ed. by B.Sunden, A.Zukauskas. Elsevier Science Publishers, 1992, 950-959.